

# Microscopic Susceptibility-Induced Steady-State Perturbation: Theory and Experiment

O. Bieri<sup>1</sup>, K. Scheffler<sup>1</sup>

<sup>1</sup>MR-Physics, Department of Medical Radiology, University of Basel, University Hospital, Basel, Basel, Switzerland

**Introduction.** Susceptibility effects in a microvascular network are the origin of the BOLD contrast, and consequently models based on a Hahn spin-echo (SE) and gradient-echo (GE) type of experiment have a long history and are profoundly investigated (1-8). Only recently the question was raised whether other type of sequences may have a better sensitivity to mesoscopic paramagnetic structures (8). Here we derive a model based on Monte Carlo simulations and experiments that describes susceptibility-based contrast in a balanced SSFP type of sequence – prototype for all steady state protocols. Susceptibility effects show up as an overall reduction in steady state amplitude that depends on the repetition time and susceptibility difference, as well as on relaxation times and on flip angle.

**Steady State Perturbation.** Figure 1A depicts a spin moving through local field inhomogeneities  $\Delta B_z$  generated by microparticles of radius  $R$ . The field perturbation (in cgs units) from a microsphere is of form

$$\Delta B_z(r, \vartheta) = \frac{4\pi}{3} \cdot \Delta\chi \cdot \left(\frac{R}{r}\right)^3 \cdot (3\cos^2\vartheta - 1) \cdot B_0$$

where  $(r, \vartheta)$  are spherical coordinates between the proton's and perturber's location and  $\Delta\chi$  is the susceptibility difference between the spheres and the surrounding medium. Diffusion in mesoscopic field inhomogeneities lead to the transition of the unperturbed steady state to a new "averaged" state  $\langle SS \rangle$ , on the order of  $T_1$  (Fig. 1B). It can be shown that perturbation effects can be incorporated into an effective steady state relaxivity  $R_{SS} \sim \xi \cdot R_2^*$ ,  $\xi \in [0 \dots 1]$ , where  $\xi$  describes the fraction of spin experiencing uncorrelated spin dephasings and  $R_2^*$  is the GE relaxivity. A simple substitution in the "normal"  $T_2$  relaxation,  $1/T_2 \rightarrow 1/T_2 + R_{SS}$  can then be used to extrapolate  $\langle SS \rangle$  to a set of other flip angles or relaxation times.

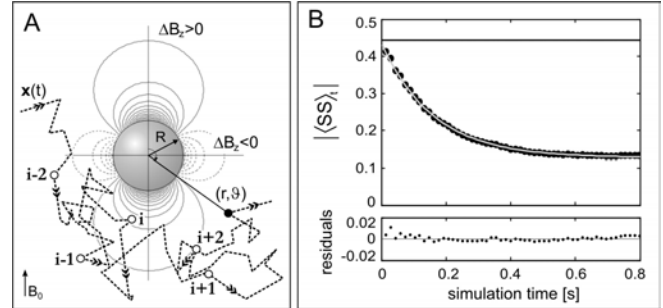


Fig. 1: (A) The bSSFP signal relaxes to a new "averaged" steady state when random motion through magnetic field inhomogeneities starts (B). The parameters are  $B_0=1.5T$ ,  $\zeta=2\%$ ,  $\Delta\chi=0.6 \times 10^{-6}$ ,  $D=2\mu m^2/ms$ ,  $R=3.5\mu m$ ,  $\Delta\chi=0.6 \times 10^{-6}$ ,  $TR=10ms$ ,  $T_1=590ms$ ,  $T_2=490ms$ ,  $\alpha=70^\circ$ .

**Methods.** (Monte Carlo Simulations) For bSSFP signal simulation Monte Carlo methods as described elsewhere (9) were combined with numerical application of 3x3 rotation and relaxation matrices, according to the piecewise constant, integrated Bloch equation (10). (Experiments) 3D bSSFP experiments were performed with a cylindrical plastic bottle filled with doped water (11mM Dy-DTPA,  $T_1=590ms$ ,  $T_2=490ms$ ) that embeds a test tube containing an equally doped  $\zeta=2\%$  dispersion of impenetrable microspheres (11mM Dy-DTPA,  $\Delta\chi=0.6 \times 10^{-6}$ ).

**Results & Discussion.** In contrast to simple GE or SE protocols, where microscopic susceptibility variations shows up as an enhanced transverse relaxation, steady state amplitude is drastically reduced (Fig. 1). This reduction is quantified by the amount

$$\Delta SS = 1 - \lim_{t \rightarrow \infty} \left( \frac{\langle SS \rangle_0}{\langle SS \rangle_t} \right)$$

and Figure 2 summarizes the effect of size ( $R$ ) and TR on  $\Delta SS$  at peak susceptibilities found during bolus passage ( $\approx 20mM$  Gd-DTPA). The shape of  $\Delta SS$  is rather similar to the well-known SE relaxivity curve. However, striking is the pronounced TR dependence of  $\Delta SS$  in the static diffusion regime (SDR), whereas in the diffusion narrowing regime (DNR)  $\Delta SS$  is virtually independent on repetition time.

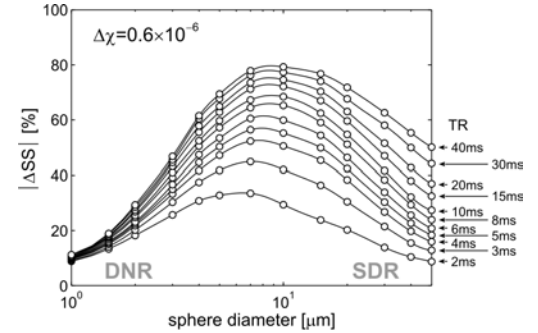


Fig. 2: Dependence of the apparent signal change  $\Delta SS$  on perturber size and TR from Monte Carlo simulations (circles) at  $\Delta\chi=0.6 \times 10^{-6}$ . The parameters are  $B_0=1.5T$ ,  $\zeta=2\%$ ,  $D=2\mu m^2/ms$ ,  $T_1=590ms$ ,  $T_2=490ms$ ,  $\alpha=70^\circ$ .

Sample images with  $TR=4ms$  are displayed on top of Fig. 3 for various radii and show an average image of the two central slices. The susceptibility induced signal loss is clearly visible in the inner tube containing microspheres. The lower panels in Fig. 3 show  $\Delta SS$  from measurements and Monte Carlo simulations. The overall dependence of  $\Delta SS$  on  $R$  and  $TR$  is evident and the very good agreement between simulation and experiment is striking. It can further be shown, that based on the Bloch-Torrey (11) equation and some general arguments on steady state systems, scaling leads to

$$t \rightarrow t/\beta, \Delta\chi \rightarrow \beta\Delta\chi, \sqrt{\beta}R \rightarrow R \Rightarrow \sqrt{\beta} \cdot \Delta SS(TR, \Delta\chi, \sqrt{\beta} \cdot R) = \Delta SS\left(\frac{TR}{\beta}, \beta \cdot \Delta\chi, R\right)$$

**Conclusion.** Reduction in steady state amplitude not only depends on micro particle properties causing the magnetic field perturbations, but also on relaxation times and sequence specific properties. Due to the high sensitivity of bSSFP type of sequences to susceptibility variations in combination with fast acquisition times and excellent SNR, steady state sequences may become an important role in susceptibility-based MRI contrast applications to quantify tissue hemodynamics, especially in the brain

**References.** [1] Ogawa S *et al.* Biophys J 1993, **64**:803-812. [2] Weisskoff RM *et al.* MRM 1994, **31**:601-610. [3] Yablonskiy DA *et al.* MRM 1994, **32**:749-763. [4] Kennan RP *et al.* MRM 1994, **31**:9-11. [5] Boxerman JL *et al.* MRM 1995, **34**:4-10. [6] Kiselev VG *et al.* MRM 1999, **41**:499-509. [7] Kiselev VG *et al.* Phys Rev Lett 2002, **89**:278101. [8] Fröhlich AF *et al.* MRM 2005, **53**:564-573. [9] Metropolis N *et al.* J Am Stat Ass 1949, **44**:335-341. [10] Hoult D. J Magn Reson 1979, **35**:69-86. [11] Torrey HC. Phys Rev 1956, **104**: 563-565.

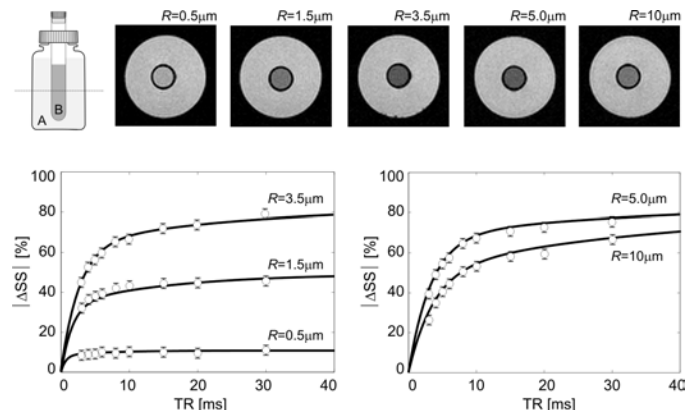


Fig. 3: A plastic bottle embeds a test tube with containing 2% microspheres (11mM Dy-DTPA,  $\Delta\chi=0.6 \times 10^{-6}$ ). Typical bSSFP images are displayed for  $TR=4ms$  and  $\alpha=70^\circ$  (top). Susceptibility related signal loss depends on size and is clearly visible in the inner tube. The lower panels show the reduction in  $\Delta SS$  from Monte Carlo simulations (solid line) and from experiments (circles).